Scripta Materialia 170 (2019) 1–5

Contents lists available at ScienceDirect

Scripta Materialia

journal homepage: www.elsevier.com/locate/scriptamat

Microstructure and dielectric property of flash sintered SiO_2-coated $BaTiO_3$ ceramics

Baisheng Ma [a], Yan Zhu [a], Kewei Wang [a], Zhenzhong Sun [a], Dianguang Liu [b], Gang Shao [c], Jinling Liu [d,*], Yiguang Wang [e,*]

[a] School of Mechanical Engineering, Neutron Scattering Technical Engineering Research Center, Dongguan University of Technology, Dongguan, Guangdong 523808, China
[b] Key Laboratory of Advanced Technologies of Materials, Ministry of Education, Southwest Jiaotong University, Chengdu, Sichuan 610031, China
[c] School of Materials Science and Engineering, Zhengzhou University, Zhengzhou, Henan 450001, China
[d] Applied Mechanics and Structure Safety Key Laboratory of Sichuan Province, Southwest Jiaotong University, Chengdu, Sichuan 610031, China
[e] Institute of Advanced Structure Technology, Beijing Institute of Technology, Haidian District, Beijing 100081, China

ARTICLE INFO

Article history:
Received 26 April 2019
Received in revised form 11 May 2019
Accepted 18 May 2019
Available online 28 May 2019

Keywords:
Flash sintering
Barium titanate
Microstructure
Dielectric property

ABSTRACT

Flash sintering method was adopted to sinter SiO_2-coated $BaTiO_3$ ceramics to lower sintering temperature and shorten sintering time. The microstructure and dielectric property of $BaTiO_3$ with different amount of SiO_2 coating were studied. Samples can be flash sintered at furnace temperatures lower than conventional sintering temperature. Though the onset flash sintering temperature increased obviously with increasing SiO_2 content, the estimated sample temperatures were found close to each other. Samples with improved density was achieved with higher SiO_2 content, but their dielectric constant decreased. Flash sintered samples with 1.5 wt% SiO_2 addition possess a fair dielectric constant with improved density.

Barium titanate ($BaTiO_3$) based ceramics are widely used in industry in fabrication of multi-layer ceramic capacitors (MLCCs), permittivity thermistors, sensors, actuators, etc. [1,2] With the development of microelectronics and the miniaturization of electronic devices, the production of nanostructured ceramics with grain size in nanometer scale is imperative. Besides, previous reports showed that fine-grained $BaTiO_3$ exhibits high breakdown strength [3,4] and postponed polarization saturation [5], which are beneficial for the capacitor applications. Therefore, a lot of work focused on the fabrication of nanostructured $BaTiO_3$ ceramics for energy storage applications. Generally, it is difficult to fabricate dense $BaTiO_3$ ceramics with grain size in nanometer scale because of the ease of grain growth of $BaTiO_3$ nanoparticles. Therefore, advanced sintering techniques (such as hot isostatic pressing [6], spark plasma sintering (SPS) [7,8], microwave sintering [9], two-step sintering [10]) or sintering additives (such as glass [11]) were utilized to control the grain growth. Previous reports indicate that glass additive shows many advantages like lowering sintering temperature [12], promoting densification [13], suppressing grain growth [14], and improving dielectric breakdown strength [15]. Therefore, $BaTiO_3$/glass nanocomposites showed great potential for high energy storage capacitor applications and gained much attentions. In general, low softening point glass is preferred, from the view of sintering, to lower sintering temperature and to suppress grain growth. But these glasses usually contain complex compositions [11,16,17], which is unfavorable in industry applications. Besides, glasses with a low softening point usually contain alkali elements and this greatly decreases their dielectric strength. SiO_2, as a common, economic glass, is one of the expected glass additives in $BaTiO_3$ ceramics due to its high breakdown strength, low loss and simple composition. However, the conventional sintering temperature of the SiO_2 added $BaTiO_3$ is as high as 1250 °C [18]. The high temperature is unfavorable for suppression of grain growth. Besides, deleterious reactions between SiO_2 and $BaTiO_3$ will occur at such high temperatures, forming either $BaTiSiO_5$ or $Ba_2TiSi_2O_8$ [19,20]. To suppress grain growth and deleterious reactions in SiO_2-$BaTiO_3$ system, two basic routes are lowering sintering temperature and shortening dwelling time. SPS and microwave sintering techniques have been utilized in the SiO_2-$BaTiO_3$ system [19]. In recent years, a so-called flash sintering technique could significantly lower sintering temperature and densify materials in seconds, under the assistance of a critical electric field/power [21]. Flash sintering technique has been demonstrated to be effective in various materials [22–27], including $BaTiO_3$ [28] and porous silica [29]. Therefore, flash sintering might be a suitable technique for preparation of nanostructured SiO_2-containing $BaTiO_3$ ceramics. In addition, previous reports demonstrated that the existence of a liquid phase sintering could effectively improve the sinterability of SiC and Al_2O_3 ceramics during flash sintering [30–32]. Inspired by these facts, the SiO_2-coated $BaTiO_3$ ceramics were flash sintered in this paper and their

* Corresponding authors.
E-mail addresses: liujinling@swjtu.edu.cn (J. Liu), wangyiguang@bit.edu.cn (Y. Wang).

https://doi.org/10.1016/j.scriptamat.2019.05.019
1359-6462/

microstructure and dielectric properties were studied. Fine-grained $BaTiO_3$ ceramics with improved density were obtained.

SiO_2 was introduced into $BaTiO_3$ powders in the form of coating by using the Stöber method [33]. $BaTiO_3$ nanopowders (99.9%, <100 nm) were purchased from Aladdin Reagent Co., Ltd. (Shanghai, China) and tetraethylorthosilicate (TEOS) was purchased from Sigma-Aldrich. The materials were used as received. Different amount (1.5 wt%, 3 wt%, 5 wt%) of SiO_2 was coated on $BaTiO_3$ nanopowders by adjusting the amount of TEOS. First, 10 g $BaTiO_3$ nanopowders were suspended in a mixture of 25 mL ethanol and 1 mL acetic by ultrasonication for 30 min and by magnetic stirring for 30 min at room temperature. Then, TEOS (the amount of TEOS was calculated according to the designed amount of SiO_2) was added into the suspension slowly and magnetic stirred for another 30 min. Subsequently, the pH value of the suspension was adjusted to ca. 9.5 by adding ammonia water solution. The obtained suspension was heated to 40 °C and maintained for at least 5 h while keeping magnetic stirring for a fully hydrolysis reaction of TEOS. At last, the SiO_2-coated $BaTiO_3$ nanopowders were centrifuged and washed by ethanol. The collected nanopowders were dried at 120 °C for 10 h in air.

The as-coated $BaTiO_3$ nanopowders were pressed into dog bone-shaped compacts by uniaxial pressing at 50 MPa and cold isostatic pressing at 300 MPa for 1 min. The compacts were pre-sintered at 600 °C for 2 h in air. A hole with a diameter of 1.6 ± 0.1 mm was then drilled on each end of the compact for electric connection. Platinum paste was painted into the holes and dried at 300 °C for 30 min serving as electrodes. Gauge section of the pre-sintered compacts was ~1.16 mm × 3.34 mm × 10 mm. Flash sintering experiments were carried out in a box furnace (KSL-1400X-A2, KJ Group, Anhui, China). The specimen was suspended into the furnace by two platinum wires via the holes and dc power was applied on the specimen through the wires by a DCP-1200 power supply (Adaptive Power System, Inc., USA). The furnace temperature was raised up at a rate of 10 °C/min and the preset voltage was applied on the specimen at 500 °C. A constant preset electric voltage of 500 V was used for all the samples. Severe local sintering phenomena occur when the preset current limit is high (typically higher than 20 mA), leading to nonuniform sintering and even break of samples. The local sintering section forms along the electric field direction. To avoid local sintering, a small preset current limit (10 mA) was set first. When the current reached the preset limit, the current was hold for 10s and then the limit was increased by 10 mA manually, holding for another 10s. Previous steps were repeated until reaching the maximum current limit (60 mA) at which the current was hold for 40s. At last, the power was cut out and the furnace temperature was decreased at a rate of −10 °C/min. Conventional sintering of the pure $BaTiO_3$ ceramics with same geometry was conducted at 1300 °C for 1 h for comparison. Fresh fracture morphologies of the sintered specimens were observed on a scanning electron microscope (SEM, JSM-7800F, JEOL, Japan). Density of the samples from the gauge section was measured by employing Archimedes' method with deionized water and the relative density was calculated (density references: $BaTiO_3$: 6.02 g/cm^3, amorphous SiO_2: 2.2 g/cm^3). X-ray diffraction (XRD) patterns of the sintered specimens were collected on a PANalytical X'pert Pro diffractometer with Cu $K\alpha$ radiation. For dielectric measurements, the gauge sections of the specimens were cut into rectangular blocks and polished to a 1-μm finish. Silver electrodes were painted onto the two major surfaces and fired at 200 °C for 30 min. Dielectric permittivity of the specimens were measured using an Alpha dielectric analyzer (Novocontrol Technologies GmbH, Germany) from −40 to 160 °C at 1 kHz.

The power dissipation of samples with different amount of SiO_2 coating as a function of furnace temperature during sintering was plotted in Fig. 1. Several peaks were shown because the current was increased step by step. Each step causes a power summit. Obviously, the onset temperature of flash sintering, which is represented by the power surge in the plot, increases with the increase of SiO_2 amount. Specifically, the addition of the SiO_2 dramatically increases the onset temperature compared with pure $BaTiO_3$ (from ca. 650 °C for pure $BaTiO_3$ to ca. 830 °C for $BaTiO_3$ with 1.5 wt% SiO_2). The effect of SiO_2 on the onset flash sintering temperature can be assigned to its effect on the sample conductivity. R. Raj [34] reported the power density at the onset of the flash sintering of various materials. These findings show that flash sintering occurs within a narrow power density range. The power dissipation is given by $E^2 \cdot G$, where E is the electric field and G is the electric conductance of the samples. Therefore, a variation in the conductivity of the samples leads to a variation in the onset flash sintering temperature [35]. In this paper, upon an increase in the SiO_2 amount, the conductivity of the samples decreases and higher temperatures are required to reach a critical power dissipation for flash sintering. As SiO_2 was added in the form of coating on the $BaTiO_3$ powders, the powders were well insulated via the SiO_2 layer. Therefore, the addition of the SiO_2 coating resulted in a dramatic increase in the onset flash sintering temperature of $BaTiO_3$. Even though, the furnace temperature for flash sintering of SiO_2-coated $BaTiO_3$ is still lower than conventional sintering temperature.

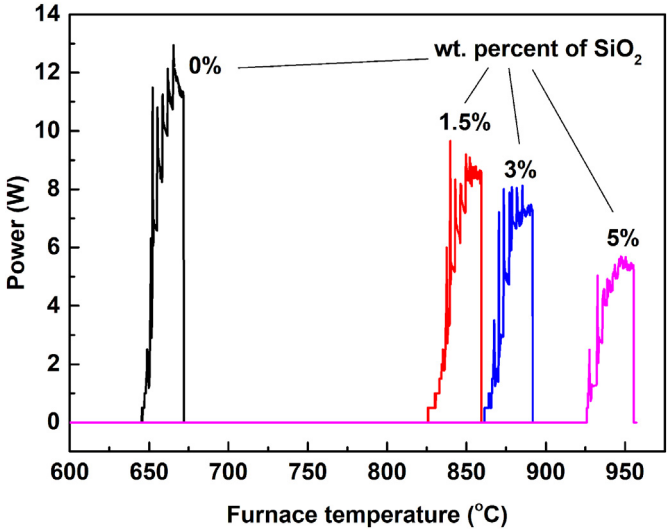

Fig. 1. Power dissipation of $BaTiO_3$ ceramics with different amount of SiO_2 coating as a function of furnace temperature.

Fig. 2 shows the microstructures of the fracture cross-sections of flash sintered $BaTiO_3$ ceramics with different amount of SiO_2. The microstructure of pure $BaTiO_3$ ceramic sintered by conventional method was also shown for comparison. A lot of pores existed within the conventional sintered pure $BaTiO_3$ (Fig. 2e). Compared with conventional sintered samples, much smaller grains were maintained in flash sintered samples (Fig. 2a). However, obvious pores can be observed in the flash sintered pure $BaTiO_3$. With increasing SiO_2 amount, the amount of pores in samples decreases and the fracture cross-section becomes more “glassy” (Fig. 2b–c). The relative density of conventional sintered pure $BaTiO_3$ measured by Archimedes' method is 95.3%. The relative densities of flash sintered $BaTiO_3$ with 0, 1.5, 3, and 5 wt% SiO_2 coating are 91.2%, 94.5%, 95.7%, and 96.1%, respectively, indicating an improvement in density with higher SiO_2 content. XRD patterns of the samples shown in Fig. 3 indicate that the flash sintered SiO_2-coated BaTiO3 ceramics contain fresnoite compound ($Ba_2TiSi_2O_8$, PDF#: 22–0513), the reactive product of SiO_2 and $BaTiO_3$. The diffraction peaks corresponding to $Ba_2TiSi_2O_8$ compound are obvious for 5 wt% SiO_2-coated $BaTiO_3$. This means that a certain amount of SiO_2 was reacted with $BaTiO_3$ during flash sintering though the sintering process was only lasting within a few minutes. The reason for the impressive reaction might be that the real temperature of the sample during flash sintering is higher than the furnace temperature because of Joule

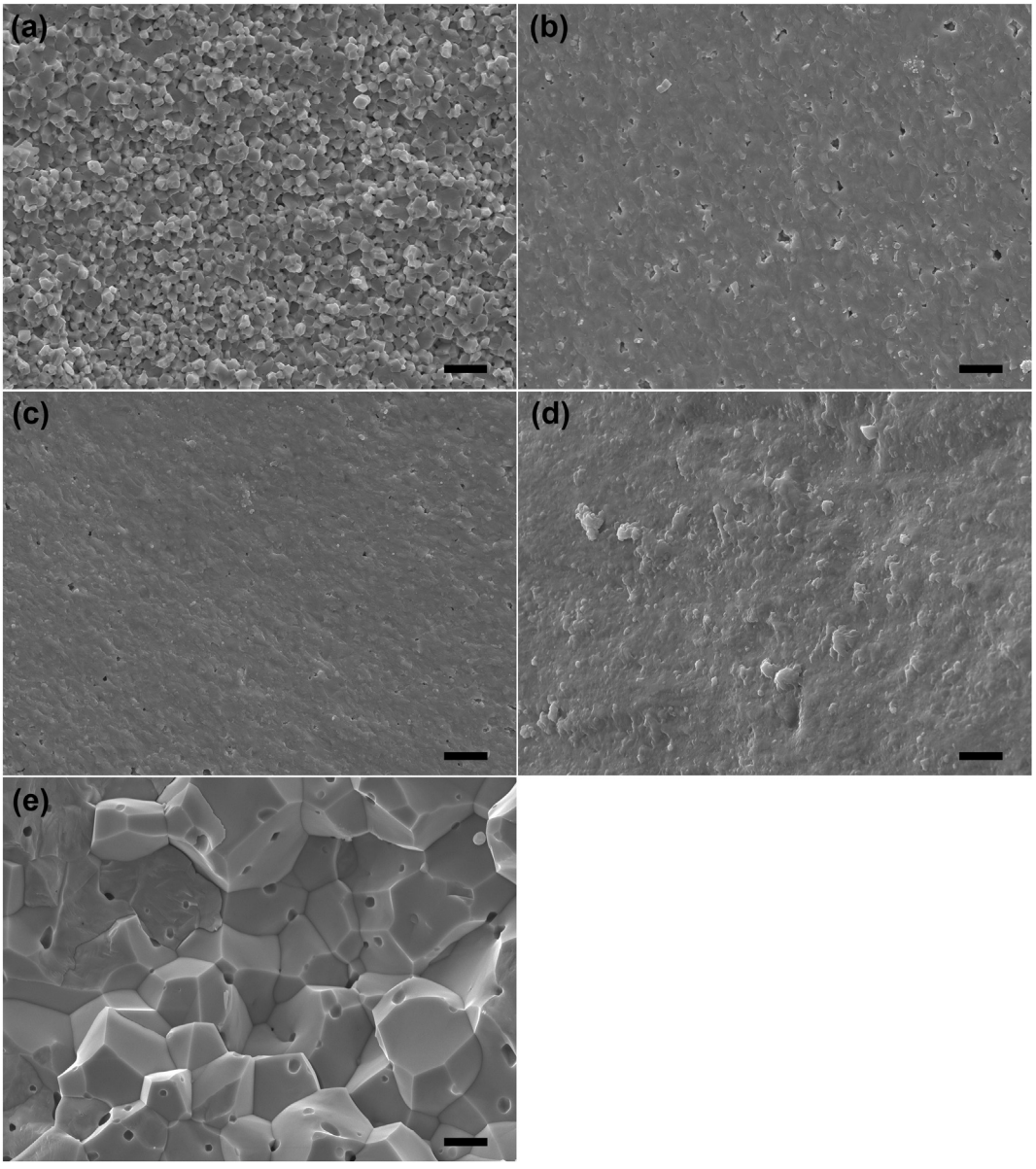

Fig. 2. Micrographs of the fracture cross-sections of flash sintered $BaTiO_3$ ceramics with (a) 0 wt%, (b) 1.5 wt%, (c) 3 wt%, (d) 5 wt% of SiO_2 coating, and of (e) conventional sintered pure $BaTiO_3$ ceramics. The scale bar in all the micrographs is 1 μm.

heating. The real temperature of the sample at the current-control stage can be estimated by using the black body radiation model when an equilibrium temperature is established. When assuming the emissivity of the samples is unity, the real sample temperature (T, in K) can be estimated by the following equation [36]:

$$T = \left[T_0^4 + \frac{W}{A\sigma}\right]^{1/4} \quad (1)$$

where T_0 is environmental (furnace) temperature in K, W is the electric energy dissipated in the sample in W, A is the surface area of the sample in m^2, and σ is a universal physical constant of 5.67×10^{-8} W m^2 K^{-4}. The power during the maximum current controlled regime and the surface area of the gauge section after sintering were used in the estimation here. (Note: the furnace temperature used in the estimation is not the onset flash sintering temperature but the temperature when the d.c. power was cut off.) The estimated temperatures for sample with 0%, 1.5%, 3%, and 5% SiO_2 coating are 1130 ± 8 °C, 1143 ± 11 °C, 1128 ± 21 °C, and 1118 ± 16 °C, respectively. The estimation results indicate that the real temperature of the samples during flash sintering is close to conventional sintering temperature. However, the sintering time here is much shorter than conventional sintering. Therefore, the reaction between SiO_2 and $BaTiO_3$ could be suppressed. Another interesting point is that even the furnace temperature of SiO_2-coated samples during flash sintering is much higher than that of uncoated samples, the estimated temperatures of these samples are similar because the power dissipation of the coated sample is lower (Fig. 1). For the same reason, the estimated temperature decreases with increasing SiO_2 content even the furnace temperature for flash sintering increases.

The dielectric constant (solid points, left-band scale) and tangent loss (hollow points, right-hand scale) of the samples at 1 kHz from −40 °C to 160 °C are presented in Fig. 4. There are two peaks in each temperature-dependence curve of the dielectric constant, which correspond to the phase transition of $BaTiO_3$. Fig. 4 shows that the SiO_2 coating can obviously suppress the dielectric anomalous peak near ferroelectric transition. The peak of the 5 wt% SiO_2-coated samples is almost disappeared. The dielectric constant of the flash sintered pure $BaTiO_3$ ceramics is much higher than that of conventional sintered

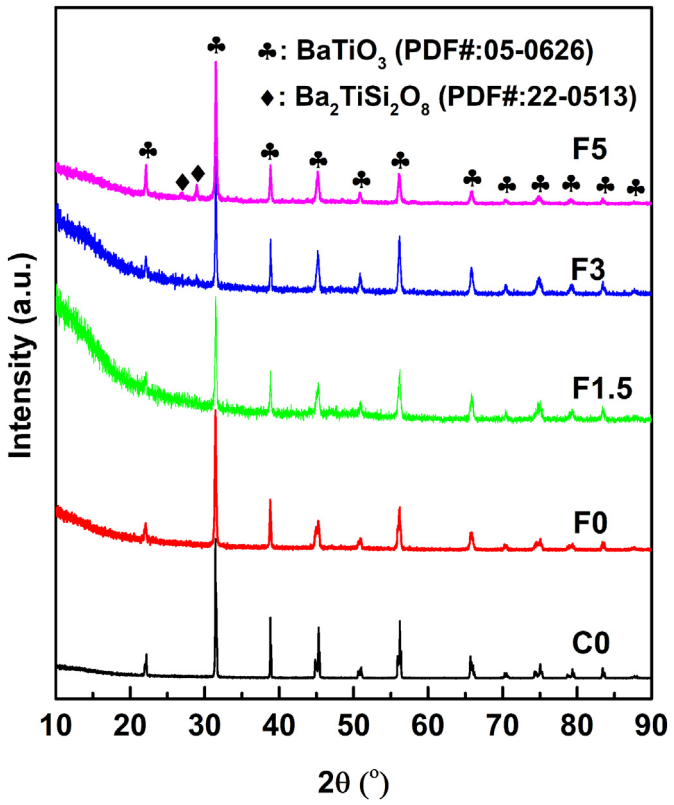

Fig. 3. XRD patterns of the sintered $BaTiO_3$-SiO_2 ceramics. C0: conventional sintered pure $BaTiO_3$; F0: flash sintered pure $BaTiO_3$; F1.5: flash sintered 1.5 wt% SiO_2-coated $BaTiO_3$; F3: flash sintered 3 wt% SiO_2-coated $BaTiO_3$; F5: flash sintered 5 wt% SiO_2-coated $BaTiO_3$.

ones. One possible reason is the difference in grain size. Previous study indicated that the dielectric constant of $BaTiO_3$ first increases and then decreases with increasing grain size from nanometer to micrometer [37]. Even though the current results are limited to demonstrate the effect of grain size in the current study, the effect of grain size cannot be excluded. Another possible reason is the defects in samples introduced by flash sintering [38]. This explanation is consistent with the result that the loss of the flash sintered pure $BaTiO_3$ is obviously higher than the conventional sintered ones. With increasing the SiO_2 amount, the dielectric constant became smaller. Still, the dielectric constant of the

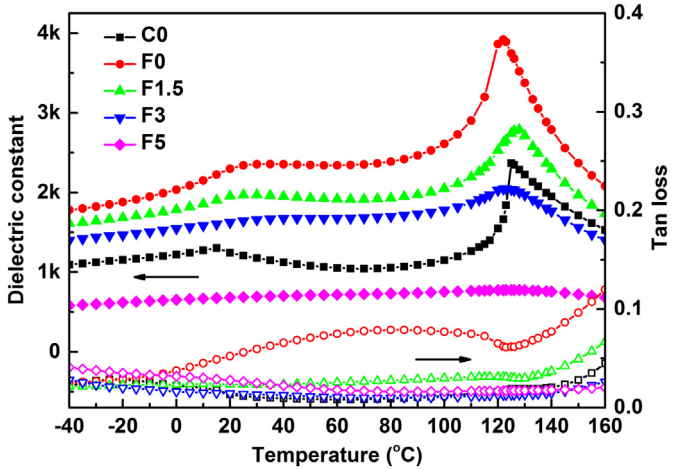

Fig. 4. Temperature dependence of dielectric constant (solid points, left-band scale) and tangent loss (hollow points, right-hand scale) of the sintered $BaTiO_3$-SiO_2 ceramics measured at 1 kHz. C0: conventional sintered pure $BaTiO_3$; F0: flash sintered pure $BaTiO_3$; F1.5: flash sintered 1.5 wt% SiO_2-coated $BaTiO_3$; F3: flash sintered 3 wt% SiO_2-coated $BaTiO_3$; F5: flash sintered 5 wt% SiO_2-coated $BaTiO_3$.

1.5 wt% SiO_2-coated samples is higher than that of conventional sintered pure $BaTiO_3$ with a reasonable dielectric loss. As for the 3 wt% SiO_2-coated samples, their dielectric constant is higher than conventional sintered pure $BaTiO_3$ at temperatures lower than the Curie temperature but is lower than the latter at temperatures higher than the Curie temperature. The dielectric constant of 5 wt% SiO_2-coated samples is smaller than that of conventional sintered pure $BaTiO_3$ and is almost independent on temperature. The Curie temperature of flash sintered pure $BaTiO_3$ (~122 °C) was lower than that of conventional sintered samples (~125 °C), which is also attributed to the difference in grain size [39]. Such phenomenon was also observed in another flash sintered undoped $BaTiO_3$ [28]. The addition of 1.5 wt% SiO_2 coating increased the Curie temperature to ~128 °C. Such increase is also reported in SPS fabricated nanostructured $BaTiO_3$/silica composites [40], where it was attributed to the existence of amorphous SiO_2 around $BaTiO_3$ grains to form a ferroelectric/dielectric composite. However, the Curie temperature of 3 wt% SiO_2-coated $BaTiO_3$ went back to ~123 °C. This variation trend of Curie temperature with SiO_2 amount was consistent with microwave sintered $BaTiO_3$/silica composites [41].

In conclusion, SiO_2-coated $BaTiO_3$ can be flash sintered at furnace temperatures lower than conventional sintering temperature. The estimated sample temperature during flash sintering was close to conventional sintering temperature, but the dwelling time for flash sintering was much shorter than conventional sintering time, which was beneficial to suppress grain growth and deleterious reactions in SiO_2-$BaTiO_3$ system. Flash sintering is demonstrated to be effective in sintering SiO_2-coated $BaTiO_3$ ceramics with improved density and fine grains.

Acknowledgements

This work was financially supported by the National Natural Science Foundation of China (Grant Nos. 51532003 and 51732009).

References

[1] A.J. Moulson, J.M. Herbert, Electroceramics: materials, properties, applications, second ed., John Wiley, Chichester, UK, 2003.
[2] R.C. Buchanan, Ceramic Materials for Electronics, third ed. Marcel Dekker, New York, 2004.
[3] H.Y. Lee, K.H. Cho, H.-D. Nam, Ferroelectrics 334 (2006) 165–169.
[4] T. Tunkasiri, G. Rujijanagul, J. Mater. Sci. Lett. 15 (1996) 1767–1769.
[5] L. Curecheriu, S.-B. Balmus, M.T. Buscaglia, V. Buscaglia, A. Ianculescu, L. Mitoseriu, J. Am. Ceram. Soc. 95 (2012) 3912–3921.
[6] G. Arlt, D. Hennings, G. de With, J. Appl. Phys. 58 (1985) 1619–1625.
[7] X. Deng, X. Wang, H. Wen, A. Kang, Z. Gui, L. Li, J. Am. Ceram. Soc. 89 (2006) 1059–1064.
[8] T. Takeuchi, M. Tabuchi, H. Kageyama, Y. Suyama, J. Am. Ceram. Soc. 82 (1999) 939–943.
[9] K. Sadhana, T. Krishnaveni, K. Praveena, S. Bharadwaj, S.R. Murthy, Scripta Mater. 59 (2008) 495–498.
[10] X.-H. Wang, X.-Y. Deng, H.-L. Bai, H. Zhou, W.-G. Qu, L.-T. Li, I.-W. Chen, J. Am. Ceram. Soc. 89 (2006) 438–443.
[11] X. Su, B.C. Riggs, M. Tomozawa, J. Keith Nelson, D.B. Chrisey, J. Mater. Chem. A 2 (2014) 18087–18096.
[12] H.-I. Hsiang, C.-S. Hsi, C.-C. Huang, S.-L. Fu, J. Alloy. Compd. 459 (2008) 307–310.
[13] A. Young, G. Hilmas, S.C. Zhang, R.W. Schwartz, J. Am. Ceram. Soc. 90 (2007) 1504–1510.
[14] J.C.C. Lin, W.-C.J. Wei, J. Electroceram. 25 (2010) 179–187.
[15] B. Liu, X. Wang, Q. Zhao, L. Li, J. Am. Ceram. Soc. 98 (2015) 2641–2646.
[16] H.-P. Jeon, S.-K. Le, S.-W. Kim, D.-K. Choi, Mater. Chem. Phys. 94 (2005) 185–189.
[17] H. Yang, F. Yan, Y. Lin, T. Wang, J. Eur. Ceram. Soc. 38 (2018) 1367–1373.
[18] Y. Zhang, M. Cao, Z. Yao, Z. Wang, Z. Song, A. Ullah, H. Hao, H. Liu, Mater. Res. Bull. 67 (2015) 70–76.
[19] D.S. Tucker, C.W. Hill, X. Zhou, G. Thompson, B. Ma, Z. Chang, Materialia 1 (2018) 46–51.
[20] X. Lu, Y. Tong, H. Talebinezhad, L. Zhang, Z.-Y. Cheng, J. Alloy. Compd. 745 (2018) 127–134.
[21] M. Biesuz, V.M. Sglavo, J. Eur. Ceram. Soc. 39 (2019) 115–143.
[22] M. Yu, S. Grasso, R. Mckinnon, T. Saunders, M.J. Reece, Adv. Appl. Ceram. 116 (2017) 24–60.
[23] D. Liu, Y. Gao, J. Liu, F. Liu, K. Li, H. Su, Y. Wang, L. An, Scripta Mater. 114 (2016) 108–111.
[24] K. Ren, J. Xia, Y. Wang, J. Eur. Ceram. Soc. 39 (2019) 1366–1373.

[25] D. Liu, Y. Gao, J. Liu, K. Li, F. Liu, Y. Wang, L. An, J. Eur. Ceram. Soc. 39 (2016) 2051–2055.
[26] J. Nie, Y. Zhang, J.M. Chan, R. Huang, J. Luo, Scripta Mater. 142 (2018) 79–82.
[27] D. Kok, S.K. Jha, R. Raj, M.L. Mecartney, J. Am. Ceram. Soc. 100 (2017) 3262–3268.
[28] J.-C. M'Peko, J.S.C. Francis, R. Raj, J. Eur. Ceram. Soc. 34 (2014) 3655–3660.
[29] M.O. Prado, M. Biesuz, M. Frasnelli, F.E. Benedetto, V.M. Sglavo, J. Non-Cryst. Solids 476 (2017) 60–66.
[30] V.M. Candelario, R. Moreno, R.I. Todd, A.L. Ortiz, J. Eur. Ceram. Soc. 37 (2017) 485–498.
[31] M. Biesuz, V.M. Sglavo, J. Eur. Ceram. Soc. 37 (2017) 705–713.
[32] J. Gonzalez-Julian, O. Guillon, J. Am. Ceram. Soc. 98 (2015) 2018–2027.
[33] W. Stöber, A. Fink, E. Bohn, J. Colloid Interf. Sci. 26 (1968) 62–69.
[34] R. Raj, J. Am. Ceram. Soc. 99 (2016) 3226–3232.
[35] B. Yoon, D. Yadav, S. Ghose, R. Raj, J. Am. Ceram. Soc. 102 (2019) 2294–2303.
[36] R. Raj, J. Eur. Ceram. Soc. 32 (2012) 2293–2301.
[37] G. Arlt, D. Hennings, G. de With, J. Appl. Phys. 58 (1985) 1619.
[38] A. Karakuscu, M. Cologna, D. Yarotski, J. Won, J.S.C. Francis, R. Raj, B.P. Uberuaga, J. Am. Ceram. Soc. 95 (2012) 2531–2536.
[39] Z. Zhao, V. Buscaglia, M. Viviani, M.T. Buscaglia, L. Mitoseriu, A. Testino, Phys. Rev. B 70 (2004), 024107.
[40] U.-C. Chung, C. Elissalde, F. Mompiou, J. Majimel, S. Gomez, C. Estournès, S. Marinel, A. Klein, F. Weil, D. Michau, S. Mornet, M. Maglione, J. Am. Ceram. Soc. 93 (2010) 865–874.
[41] Y. Yan, L. Liu, C. Ning, Y. Yang, C. Xia, Y. Zou, S. Liu, X. Wang, K. Liu, X. Liu, G. Liu, Mater. Lett. 165 (2016) 135–138.